Current Climate Vulnerability Map, Water Supply, Distribution and Consumptive Use

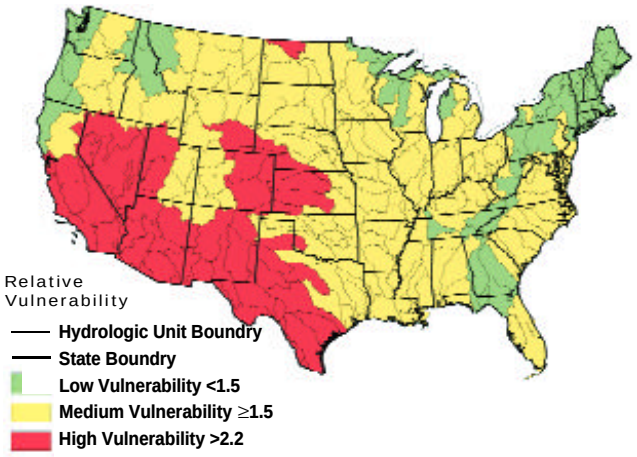

Figure 2: Assessed vulnerability based on current climate and water resource conditions, based on data describing the following: share of streamflow withdrawn for use, streamflow variability, evapotranspiration rate, groundwater overdraft, industrial use savings potential, and water trading potential. Source: Hurd, B.J., N. Leary, R. Jones and J. Smith. (1999a).

Observed Changes In Streamflow and Precipitation (1939-99)

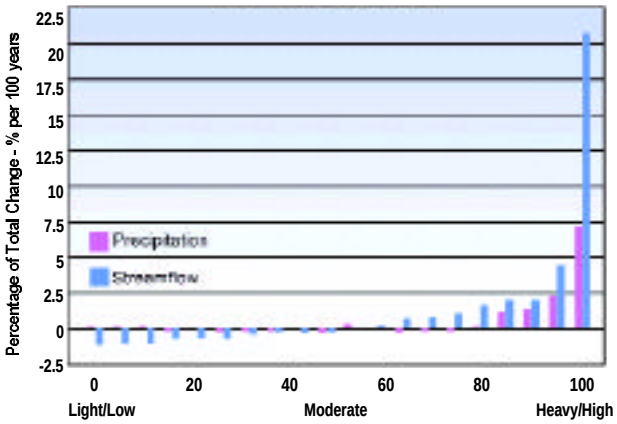

Figure 5: The graph shows changes in the intensity of precipitation and streamflow, displayed in 5% increments, during the period 1939-99 based on over 150 unregulated streams across the US with nearby precipitation measurements. As the graph demonstrates, the largest changes have been the significant increases in the heaviest precipitation events and the highest streamflows. Note that changes in streamflow follow changes in precipitation, but are amplified by about a factor of 3. Source: Groisman, et.al. (2001).

Current Climate Vulnerability Map, Instream Use, Water Quality and Ecosystem Support

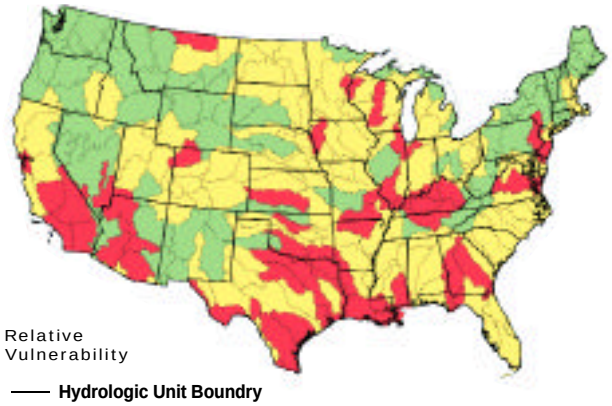

Figure 19: Instream Use, Water Quality, and Ecosystem Support Assessed Vulnerability based on current climate and water resource conditions, based on data describing the following: flood risk population, navigation impacts, ecosystem tolerance to cold and heat, dissolved oxygen stress, low streamflow conditions, and number of aquatic species at risk. Source: Hurd, B.J., N. Leary, R. Jones and J. Smith, 1999a. (Duplicated on Page 600)

Projected 21st Century Change in US Daily Precipitation

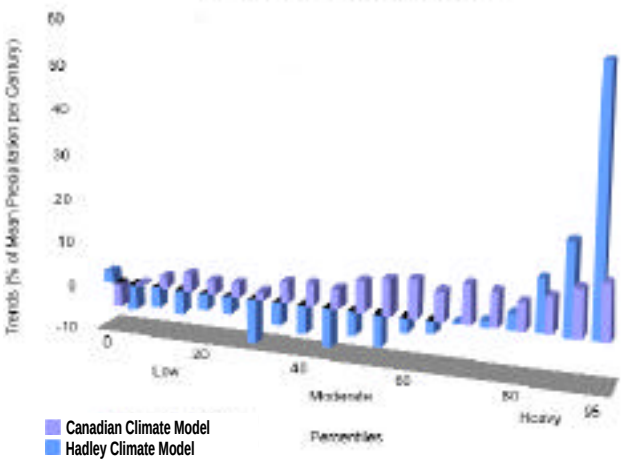

Figure 6: These projections from the Hadley and Canadian models show the changes in precipitation over the 21st century. Each models' projected change in the lightest 5% of precipitation events is represented by the far left bar and the change in the heaviest 5% by the far right bar. As the graph illustrates, both models project significant increases in heavy rain events with smaller increases or decreases in light rain events. Source: National Climatic Data Center.

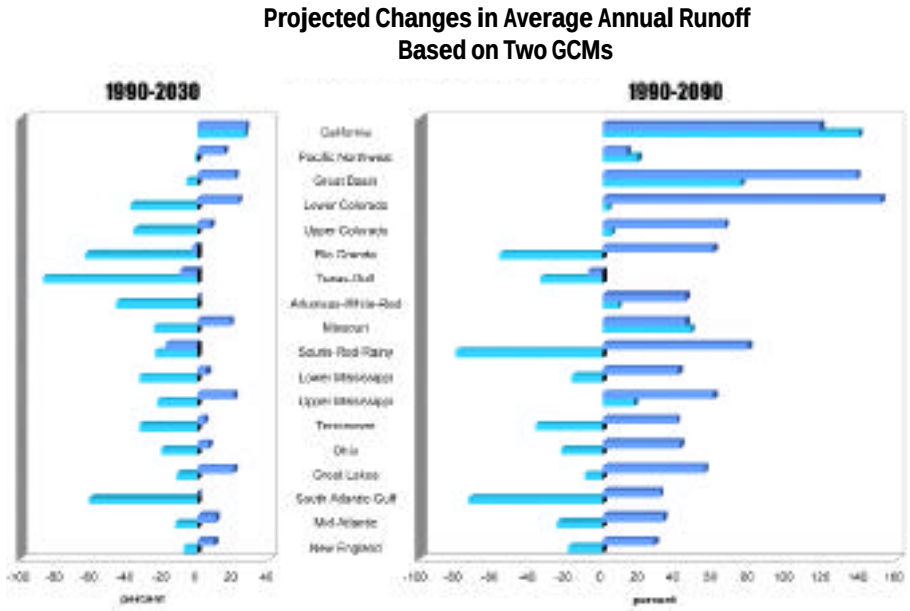

Figure 7: The estimated percent changes in average annual runoff based on the Canadian and Hadley models are not well correlated. The Canadian model predicts declines in runoff in all regions except California, while the Hadley model projects increases in most regions, particularly in the Southwest. The models differ in precipitation predictions in part due to underlying model construction. Source: Wolock, D.M. and G.J. McCabe, 1999a.

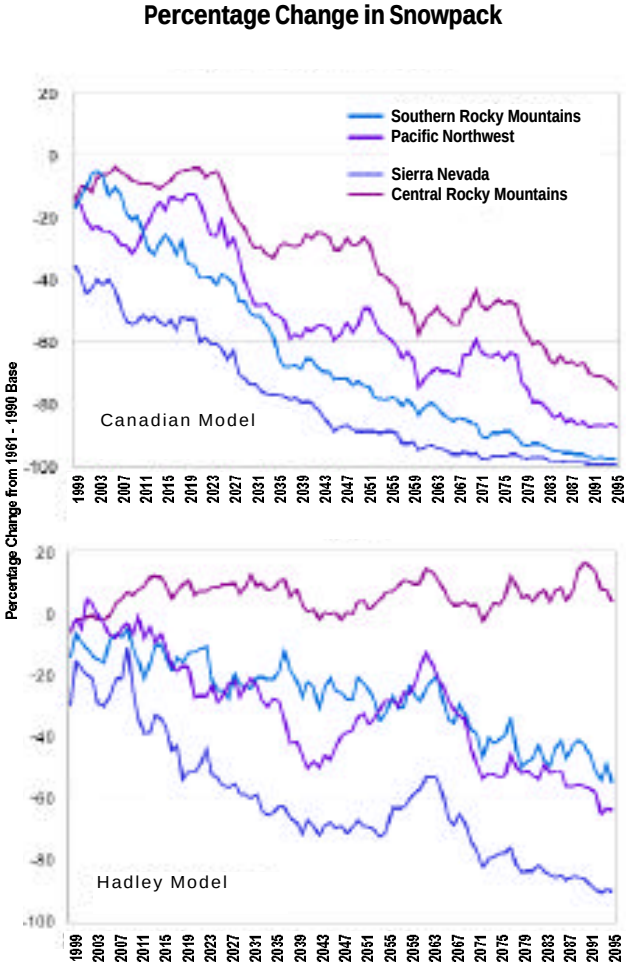

Figure 8: Percentage change from the 1961-90 baseline in the April 1 snowpack in four areas of the western US as simulated for the 21st century by the Canadian and Hadley models. April 1 snowpack is important because it stores water that is released into streams and reservoirs later in the spring and summer. The sharp reductions are due to rising temperatures and an increasing fraction of winter precipitation falling as rain rather than snow. The largest changes occur in the most southern mountain ranges and those closest to the warming ocean waters. Source: McCabe, G.J. and D.M. Wolock. 1999.

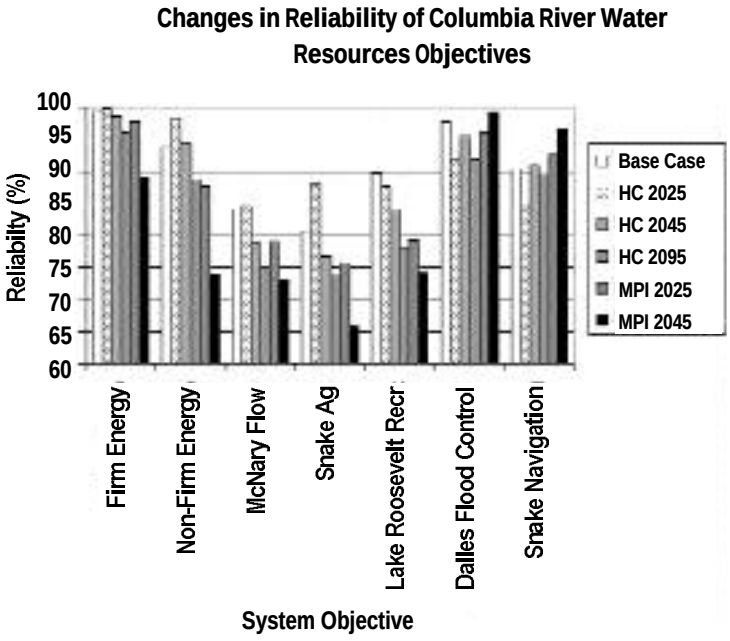

Figure 9: Four major objectives are impacted by low summer streamflow and reservoir storage: non-firm energy production; irrigation; instream flow; and recreation at Lake Roosevelt. Source: Hamlet, A.F. and D.P. Lettenmaier.

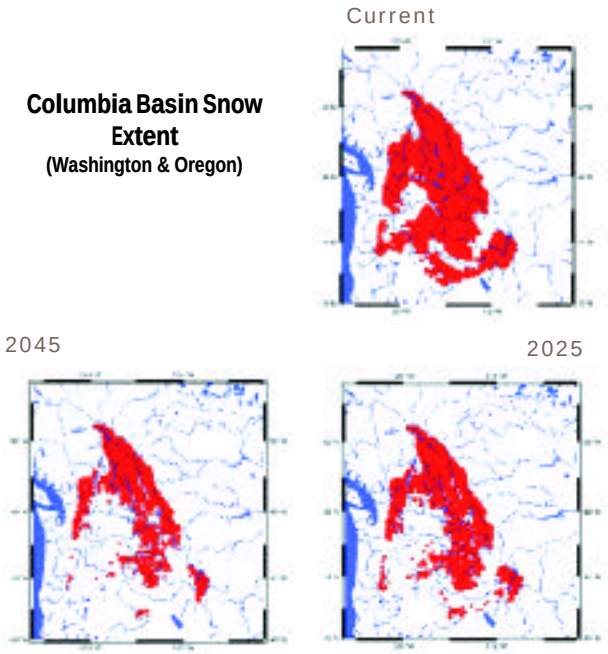

Figure 11: Complete loss of snow cover is projected at lower elevations. These maps are generated by downscaling output from global to regional climate models. Output shown from these models relates to the Columbia Basin; no projections are included for the blank areas outside the basin. Source: Mote, et.al.,(1999) Impacts of climate variability and change in the Pacific Northwest, University of Washington.

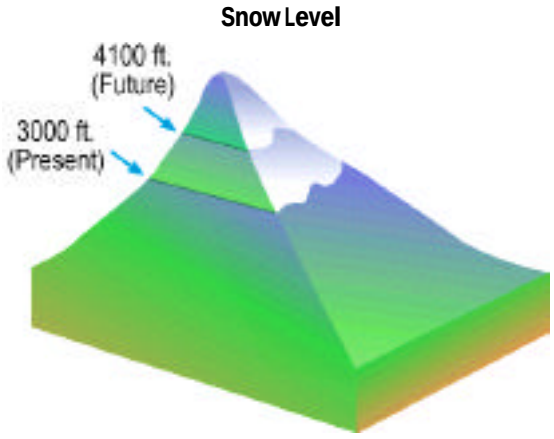

Figure 10: Rough estimate of how much snowlines in the Pacific Northwest are likely to shift by 2050, assuming about 4ºF warming. Source: R. Leung, Pacific Northwest National Laboratory.

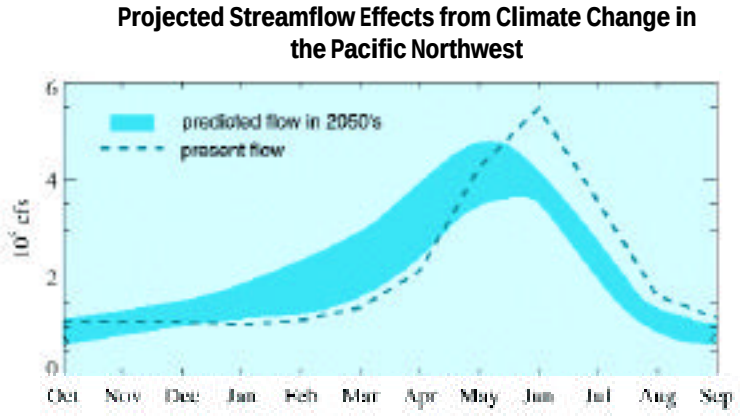

Figure 12: Relative to present flows (dashed), the wetter winters and drier summers simulated by climate models are very likely to shift peak streamflow earlier in the year, increasing the risk of late-summer shortages. Though the Columbia system is only moderately sensitive to climate change, allocation conflicts and a cumbersome network of interlocking authorities restrict its ability to adapt, producing substantial vulnerability to these shortages. Source: Hamlet, A.F. and D.P. Lettenmaier. 1999.

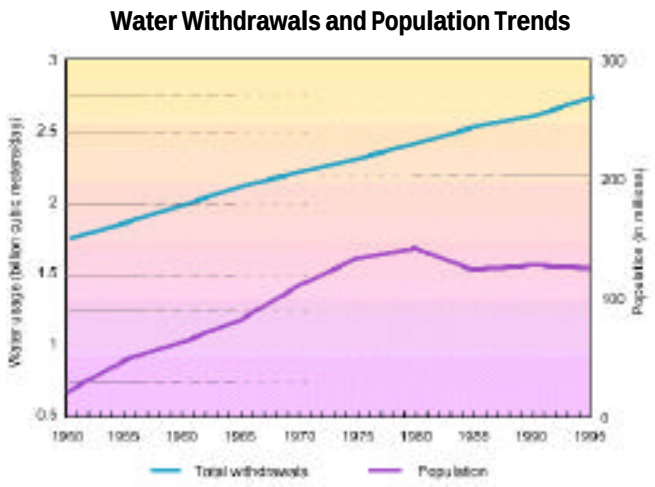

Figure 13: Although US population has continued to increase, withdrawals have declined on a per capita basis. Reductions are due to increased efficiency and recycling in some sectors, and a reduction in acreage of irrigated agriculture. Source: Solley, W.B., R.R. Pierce, and H. A.Perlman, 1998.

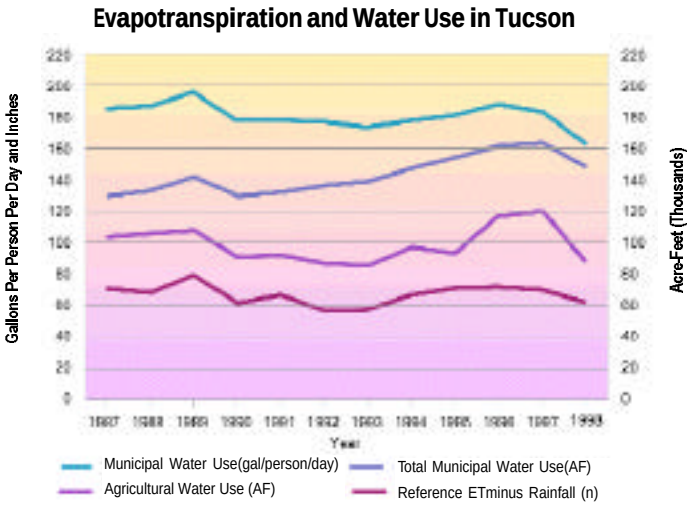

Figure 15: Water demand in the agricultural and municipal water use sectors correlates strongly with evapotranspiration rates. Source: Arizona Deptartment of Water Resources.

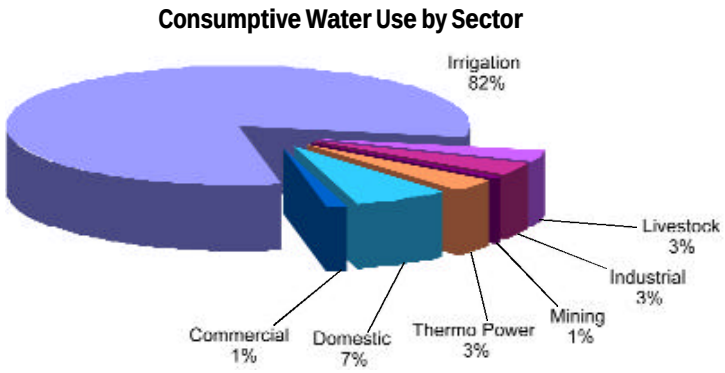

Figure 14: Agricultural water use is the highest consumptive use sector. Source: Data from Solley, W.B., R.R. Pierce, and H. A.Perlman, 1998.

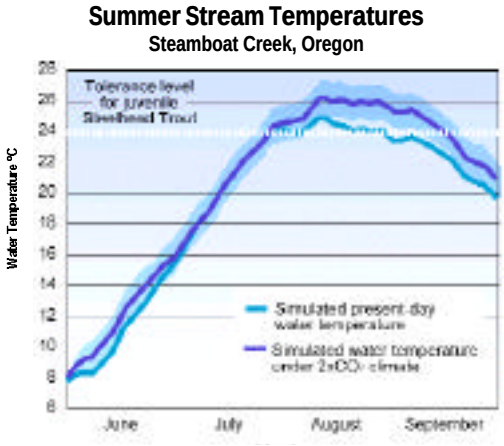

Figure 18: Simulated summer stream temperatures under present day climate (blue) and simulated temperatures under about a twice current CO_2 climate (red). The dashed line at 24 ºC (75 ºF) on the "water temperature" axis indicates the summer temperature tolerance of juvenile steelhead trout. Under doubled CO_2, the model suggests that the length of time within the year when the temperature tolerance limit is exceeded is more than twice as long as under simulated present-day climate conditions. Shaded area surrounding the doubled CO_2 temperature curve indicates an estimate of uncertainty.

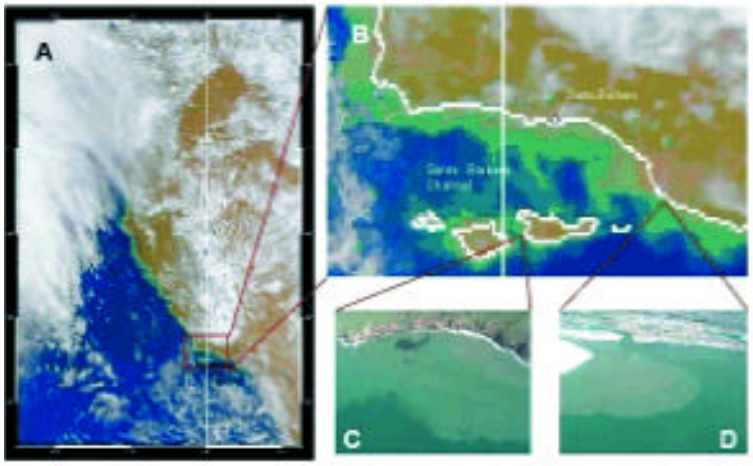

Figure 16: Sediment flow off Santa Barbara caused by El Niño storm runoff. Source: Mertes, L., The Plumes and Blooms Project, ICESS/UCSB.

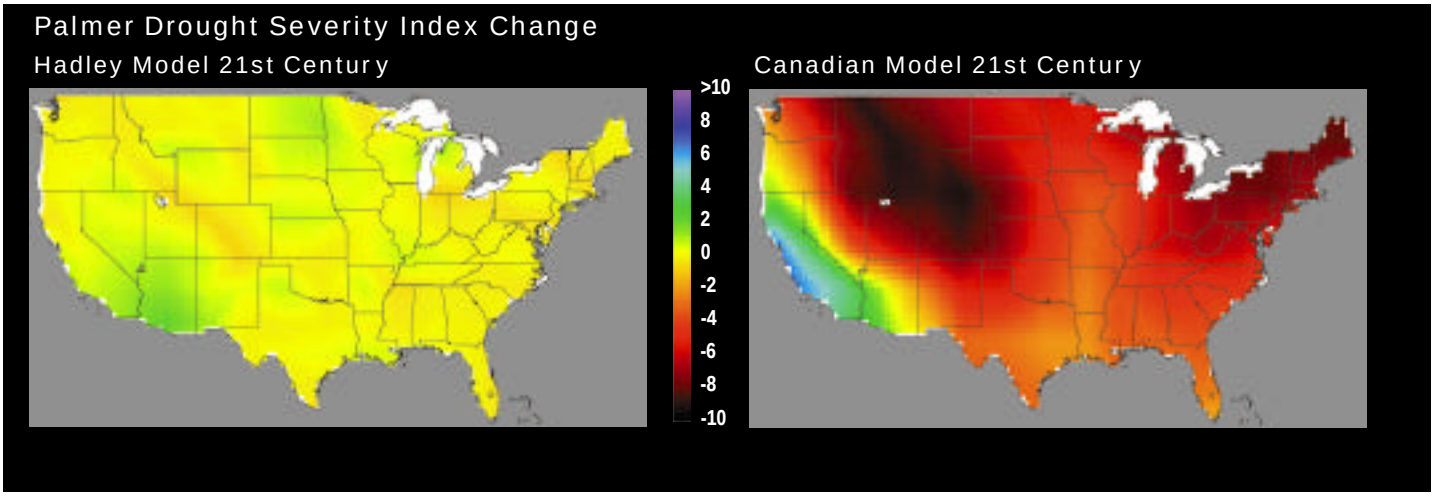

Figure 24: The Palmer Drought Severity Index (PDSI) is a commonly used measure of drought severity taking into account differences in temperature, precipitation, and capacity of soils to hold water. These maps show projected changes in the PDSI over the 21st century, based on the Canadian and Hadley climate scenarios. A PDSI of -4 indicates extreme drought conditions. The most intense droughts are in the -6 to -10 range, similar to the major drought of the 1930s. By the end of the century, the Canadian scenario projects that extreme drought will be a common occurrence over much of the nation, while the Hadley model projects much more moderate conditions. Source: Felzer, B. UCAR.

Current Climate Vulnerability Map, Instream Use, Water Quality and Ecosystem Support

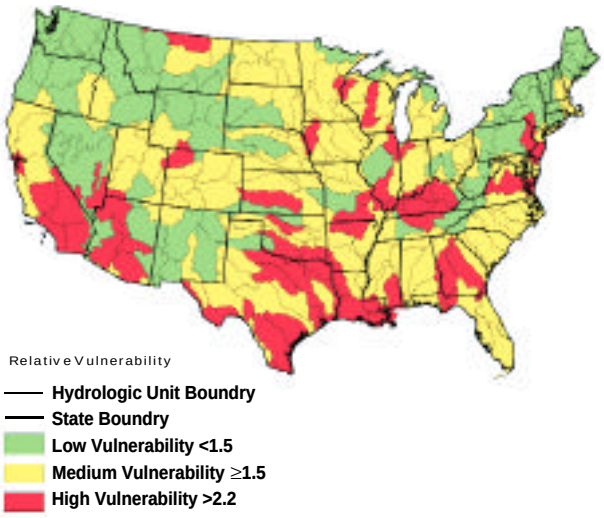

Figure 19: Instream Use, Water Quality, and Ecosystem Support Assessed Vulnerability based on current climate and water resource conditions, based on data describing the following: flood risk population, navigation impacts, ecosystem tolerance to cold and heat, dissolved oxygen stress, low streamflow conditions, and number of aquatic species at risk. Source: Hurd, B.J., N. Leary, R. Jones and J. Smith, 1999a.